NIH Public Access
Author Manuscript
J Pain. Author manuscript; available in PMC 2014 October 01.

Published in final edited form as:
J Pain. 2013 October ; 14(10): 1077–1087. doi:10.1016/j.jpain.2013.04.003.

Functional Connectivity of the Default Mode Network and Its Association With Pain Networks in Irritable Bowel Patients Assessed via Lidocaine Treatment

Janelle E. Letzen[*], **Jason G. Craggs**[*], **William M. Perlstein**[*,†,‡], **Donald D. Price**[§], and **Michael E. Robinson**[*]

[*]Department of Clinical and Health Psychology, University of Florida, Gainesville, Florida

[§]Department of Oral and Maxillofacial Surgery, University of Florida, Gainesville, Florida

[†]VA RR&D Brain Rehabilitation Research Center of Excellence, Malcom Randall VA, Gainesville, Florida

[‡]McKnight Brain Institute, University of Florida, Gainesville, Florida

Abstract

The default mode network (DMN), a group of brain regions implicated in passive thought processes, has been proposed as a potentially informative neural marker to aid in novel treatment development. However, the DMN's internal connectivity and its temporal relationship (ie, functional network connectivity) with pain-related neural networks in chronic pain conditions is poorly understood, as is the DMN's sensitivity to analgesic effects. The current study assessed how DMN functional connectivity and its temporal association with 3 pain-related networks changed after rectal lidocaine treatment in irritable bowel syndrome patients. Eleven females with irritable bowel syndrome underwent a rectal balloon distension paradigm during functional magnetic resonance imaging in 2 conditions: natural history (ie, baseline) and lidocaine. Results showed increased DMN connectivity with pain-related regions during natural history and increased within-network connectivity of DMN structures under lidocaine. Further, there was a significantly greater lag time between 2 of the pain networks, those involved in cognitive and in affective pain processes, comparing lidocaine to natural history. These findings suggest that 1) DMN plasticity is sensitive to analgesic effects, and 2) reduced pain ratings via analgesia reflect DMN connectivity more similar to pain-free individuals. Findings show potential implications of this network as an approach for understanding clinical pain management techniques.

Perspective—This study shows that lidocaine, a peripheral analgesic, significantly altered DMN connectivity and affected its relationship with pain-related networks. These findings suggest that the DMN, which is hypothesized to represent non-goal-oriented activity, is sensitive to analgesic effects and could be useful to understand pain treatment mechanisms.

Keywords

Default mode network; fMRI; irritable bowel syndrome; lidocaine; functional network connectivity

© 2013 by the American Pain Society

Address reprint requests to Michael E. Robinson, PhD, University of Florida, 101 South Newell Dr, Rm 3151, PO Box 100165, Gainesville, FL 32610-9165. merobin@ufl.edu.

The authors have no conflict of interest to declare.

NIH-PA Author Manuscript
NIH-PA Author Manuscript
NIH-PA Author Manuscript

NIH-PA Author Manuscript

NIH-PA Author Manuscript

NIH-PA Author Manuscript

Alterations in functional brain connectivity have been found across a variety of chronic pain populations.[7,35,37] Although early functional magnetic resonance imaging (fMRI) studies of chronic pain focused on coactivated brain regions during specific tasks, such as the processing of experimental pain, recent studies have examined how activity among task-negative neural networks influences the experience of chronic and experimental pain.[38] One such network, the default mode network (DMN), has been hypothesized to potentially help highlight the complexities of pain mechanisms.[10] The DMN is a set of cortical regions that have greater coherence of neural activity during rest (ie, when an individual is not actively engaged in a goal-directed task, such as self-referential mental activity[19] and mindwandering[6]), or task-negative periods during an experimental protocol. Moreover, because patients have exhibited DMN activity even under anesthesia, the DMN has been considered a representative of baseline brain activity.[12]

Research has shown that chronic pain is associated with abnormal connectivity patterns among DMN regions. For example, Tagliazucchi and colleagues[40] found increased functional connectivity of the DMN with the insular cortex in chronic back pain patients, suggestive of an interaction between persistent pain and emotional processes during rest. Increased DMN connectivity with pain- and emotion-related brain regions have also been reported in fibromyalgia[32] and irritable bowel syndrome (IBS) patients.[20,41] Recent reviews have also proposed that the integrity of the DMN could serve as a potential marker of treatment effects for chronic pain, with implications for analgesic development.[1,32,45] However, there is little research on how current analgesics affect neural activity in the DMN, and none of the aforementioned studies has reported on the temporal relationship (ie, functional network connectivity [FNC]) between the DMN and pain-related neural networks.

To our knowledge, only 1 study has reported on the FNC between the DMN and pain-related neural networks. Otti and colleagues[33] showed that patients with somatoform pain disorder had 2 distinct pain-related networks and 2 subsystems of the DMN. Although the overall FNC pattern of these networks was not significantly different between the somatoform pain disorder and control groups, the authors suggested that their results might have been affected by the use of psychotropic medications in the patients with somatoform pain disorder because medication has been shown to alter DMN connectivity in clinical populations.

Few studies have reported treatment effects on abnormal DMN activity resulting from chronic pain. To address this need, the present study examined the effects of a peripheral analgesic, intrarectal lidocaine, on the neuronal coherence of the DMN in patients with IBS. Additionally, we examined the temporal relationship between the DMN and pain-related networks to determine whether the administration of lidocaine altered the FNC between these networks. Based on studies that reported the restorative effects of medication on the DMN in other clinical populations,[25,34,36] we predicted that after lidocaine administration, 1) functional connectivity among DMN structures would more closely resemble pain-free individuals and 2) the temporal relationships among the DMN and pain-related networks would be significantly faster.

Methods

The present work is a secondary data analysis from a study investigating the effects of rectal lidocaine (RL) on pain in patients with IBS.[9] Although the original study was a double-blind clinical trial involving 3 sessions of fMRI data collection (ie, baseline, placebo, RL), only 2 of these conditions were included in the present analyses. The current study uses a within-subjects design to examine task-negative related functional brain connectivity during 2

NIH-PA Author Manuscript

NIH-PA Author Manuscript

NIH-PA Author Manuscript

conditions in which participants were exposed to a clinically relevant pain protocol designed to emulate visceral pain experienced by IBS patients (ie, rectal distention). The first is a baseline, or natural history (NH), condition during which the rectal balloon was coated with a saline gel prior to insertion. In the second, RL condition, the rectal balloon was coated with lidocaine gel prior to insertion to produce peripherally induced analgesia. This study was approved by the University of Florida and Gainesville Veterans Administration Institutional Review Boards and performed at the University of Florida McKnight Brain Institute in Gainesville, Florida. Prior to enrollment, all participants completed an informed consent form stating that they would receive either an active analgesic (ie, lidocaine) or a placebo agent during the treatment sessions.

Participants

MRI data from 11 female patients with IBS were used in this study (mean age = 31.26 years, SD = 7.55 years). Eight participants were Caucasian, 2 were African American, and 1 was Hispanic. Inclusion criteria for the study were 1) persistent spontaneous pain for at least 6 months, 2) a diagnosis of IBS based on Rome II criteria with the exclusion of organic disease,[23] 3) no history of medical or psychological comorbidities other than those closely related to IBS (eg, major depression and anxiety), and 4) the discontinued use of pain medications, serotonin uptake inhibitors, serotonin antagonists, or tricyclic antidepressants at the time of the study. All patients were required to fast 12 hours before each MRI session and self-administered 1 Fleets enema (CB Fleet Co, Inc, Lynchberg, VA) at least 2 hours prior to the session, which was confirmed by the gastroenterologist who administered the rectal balloon distension paradigm.

Experimental Materials

To induce visceral pain, we used a clinically relevant rectal balloon distention paradigm.[42] A visceral stimulator (Metronics, Minneapolis, MN) delivered distensions to the rectal balloon at a rapid rate (870 mL/min) and constant pressure plateau between 10 and 55 mm Hg. Pressure, volume, and compliance measures were simultaneously monitored and recorded.[28,31,46] The balloon was a 500-mL polyethylene bag secured on a rectal catheter (Zinetics Medical, Inc, Salt Lake City, UT) using unwaxed dental floss and parafilm (American National Can, Greenwich, CT) to ensure a tight seal. For both conditions, the balloon was lubricated (Surgilube, E. Fougera and Co, Melville, NY) and placed into the rectum by a gastroenterologist. The balloon was inserted 4 cm from the anal sphincter to stimulate approximately 4 cm of the rectum during the inflation period. The gastroenterologist who performed study procedures was the physician with whom the majority of the patients normally consulted in the clinic. In contrast to the NH condition, which used a lubricating saline gel, during the RL condition, 300 mg of lidocaine gel (Astra USA, Inc, Westborough, MA) was applied to the entire area of the rectum that would be distended. All fMRI runs took place within 15 minutes of the lidocaine gel's effectiveness, to ensure that patients received analgesic effects throughout data collection.

Experimental Procedures

During each testing session, patients were greeted in the waiting room at the gastroenterology clinic, escorted to an examination room, and introduced to study procedures. Then, each patient's response to visceral stimuli was tested using different amounts of balloon distension pressure applied in ascending order (ie, 10, 20, 30, 40, and 50 mm Hg). Patients rated their pain after each stimulus using a pain rating scale of 0 to 100, where 0 represented "no pain" and 100 represented "the most intense pain imaginable."[43] Once a pain rating of 40 or above was reached, the corresponding pressure was recorded for use during the fMRI scans. All patients rated their pain above 40 for at least 1 of the distension pressures, and therefore none of the patients was excluded.

NIH-PA Author Manuscript

NIH-PA Author Manuscript

NIH-PA Author Manuscript

Patients completed 3 MRI sessions with no more than 1 week between each session. The first session for all patients was the NH condition, during which they were informed that treatment would not be used. In the subsequent 2 sessions, the RL condition was counterbalanced with a placebo condition, wherein either lidocaine gel or saline gel was administered on a double-blind basis. Prior to the start of scanning, patients were informed that they would receive either lidocaine or saline gel. The patients were not given any auditory or visual clues that they were to receive a stimulus. To maintain consistency in pain sensitivity across sessions, patients were only scanned on days when their spontaneous, ongoing abdominal pain ratings were at least 30.

Data Acquisition and Image Preprocessing

All structural and functional MRI data were collected using a research-dedicated head scanner with a standard 8-channel radiofrequency head-coil (Siemens Allegra, 3.0 T; Siemens, Erlangen, Germany). Each MRI session included collection of a high-resolution 3-dimensional (3D) structural image, followed by 7 fMRI scans. The high-resolution 3D anatomical images were acquired using a T1-weighted MP-RAGE protocol with the following parameters: 128 1-mm axial slices; repetition time (TR) = 2000 ms, echo time (TE) = 4.13 ms, flip angle (FA) = 8°, matrix = 256 × 256 mm, field of view (FOV) = 24 cm. Functional images were acquired from a T2-gradient echo planar imaging sequence using 33 contiguous axial slices of the whole brain parallel to the anterior commissure–posterior commissure (AC–PC) plane. Additional parameters included TR/TE = 2,000 ms/30 ms, FA = 90°, FOV = 240 × 240 mm, matrix = 64 × 64; 3.75 mm^3 isotropic voxels with .4-mm-slice gap. The stimulus onset of all fMRI scans was TR time-locked to the onset of scan acquisition. Each scan lasted for 44 seconds, during which the first 24 seconds were a rest period followed by 20 seconds of noxious rectal distension. Immediately after each fMRI scan, patients provided ratings of pain and unpleasantness using a verbal rating (Fig 1).

To reduce saturation effects from an inhomogeneous B_0 field, the first 2 volumes of each functional run were discarded at the scanner and 2 additional volumes were discarded during preprocessing. Image preprocessing was carried out using AFNI (http://afni.nimh.nih.gov/afni/) and consisted of temporal concatenation of the fMRI scans for each subject, 3D motion correction (motion censor limit = .3 mm per TR), spatial smoothing (full width at half maximum = 4 mm), slice scan time correction, and spatial normalization to a standardized MNI template.

To examine the possibility that movement artifacts might have on subsequent analyses, we examined the movement parameters and found that average displacement was less than the 2-mm-voxel dimension (NH = 1.615 mm, RL = 1.675 mm). Analysis of condition-related effects did not reveal any significant differences (NH = .124, RL = .129; $P > .05$) in movement, suggesting that observed condition-level differences in activation were not due to systematic differences in head movement.

Independent Component Analysis

The initial network analysis for this study was done with the Group ICA of fMRI Toolbox (GIFT v1.3 b; http://icatb.sourceforge.net/) for Matlab v7. ICA is a data-driven statistical analysis technique that yields independent components (ICs), which isolate sources of variance within the data. Each estimated IC represents a group of brain regions with a unique pattern of synchronized neural activity (ie, time course) and can be conceptualized as a neural network.[3] The GIFT IC estimation procedure occurs in 3 stages: 1a) reduction of data dimensionality and 1b) estimation of the optimal number of components using the MDL algorithm (22 for this study), 2) estimation of group signal sources and reduction of

NIH-PA Author Manuscript

NIH-PA Author Manuscript

NIH-PA Author Manuscript

mutual information among those sources, and 3) back reconstruction of group-level ICs to single-subject level.

Condition-Level Analyses

Following the back reconstruction of the estimated group-level ICs, each participant's ICs from both conditions were correlated with the DMN template provided by the GIFT toolbox to identify the IC that best represented the DMN. Once the IC representing the DMN in each condition was identified, we used NeuroElf (http://neuroelf.net/) to conduct a paired samples t-test to identify significant spatial differences in the ICs representing the DMN in each condition (ie, NH and RL) with the following criteria: $P \leq .01$ (corrected for family-wise error) and a minimum cluster size of 30 contiguous voxels (ie, 810 μL).

FNC

Although each IC represents a network of brain regions with a specific temporal pattern over the course of the fMRI scan (ie, time course), correlations can exist among the time courses of different ICs. In addition to producing a spatial map of each IC, GIFT outputs each IC's time course. This output shows a waveform, which represents fluctuations in the IC's activity over time, and correlations among the ICs' time courses are calculated based on the pattern of each IC's waveform. Moreover, temporal lags between ICs can be estimated to test the presence of a significant relationship between the onsets of the ICs' waveforms.[21] These temporal relationships were assessed with an extension of GIFT, the Functional Network Connectivity Toolbox (FNC; http://mialab.mrn.org/software/#fnc), an extension of GIFT.

To better understand the dynamic relationship between the DMN and pain processes, we also identified 3 distinct pain-related ICs (ie, sensation, affect, cognition). We examined all of the ICs that were output from GIFT and discovered 3 ICs with time courses that matched the study's design. Upon examining the brain regions included in each of these 3 ICs, we determined which pain-related network was the best fit, based on inclusion of brain regions described by prior literature as being associated with each respective pain process. Using the FNC toolbox, we examined 1) correlations among all 4 ICs' time courses and 2) the amount of delay between time courses (ie, lag values) in each condition. As Jafri and colleagues[21] described, we applied a band-pass Butter-worth filter for frequencies between .03 Hz and .37 Hz to each IC to detect significant condition-level changes in the cross-correlation coefficients based on sub-TR variability of the hemodynamic response. All within-condition pairwise combinations were computed via the maximal lagged correlation algorithm and tested using a 1-sample t-test ($P \leq .05$). Condition-based differences in FNC were tested via a 2-tailed paired-samples t-test ($P \leq .05$), corrected for multiple comparisons (false discovery rate [FDR][15] = .05).

Results

Pain Rating Results

To examine whether the lidocaine gel resulted in the reduction of pain, we conducted a 2-tailed paired-samples t-test of the patients' pain ratings collected during the fMRI sessions. There was a significant difference between pain ratings in the NH (= 47.82, SD = 13.212) compared to the RL (= 32.55, SD = 17.489) condition, $t(10) = 2.235$, $P \leq .05$. These results confirm that the peripheral analgesic, RL, significantly decreased patients' pain in response to rectal distension.

NIH-PA Author Manuscript

NIH-PA Author Manuscript

NIH-PA Author Manuscript

Lidocaine-Related Changes in DMN Connectivity

Among the ICs identified by the GIFT toolbox, the DMN was readily detectable by its high correlation with the GIFT template of the DMN in both the NH and RL conditions (r = .36 and r = .40, respectively). A paired-samples t-test of the DMN spatial maps revealed a significant difference in the spatial extent of the DMN in each condition ($P \leq .05$, FDR ≤.05, cluster threshold = 189 μL). Evaluation of the NH spatial map of the DMN included the insula and precentral gyrus, indicating that the activity in these pain-related regions had increased coherence with basal brain activity, which was not seen in the RL condition. Conversely, the RL spatial map of the DMN included the superior and middle temporal gyri, angular gyrus, and inferior parietal lobule, compared to NH. See Table 1 and Fig 2 for details.

Functional Network Connectivity Between the Default Mode and Pain Networks

In addition to the DMN, we identified 3 pain-related components (ICs) for both conditions: 1) a sensorimotor network (SMN), 2) an insular salience network (ISN), and 3) a cognitive control network (CCN). The waveforms in Fig 3 depict each IC's activation pattern over time (ie, time course) during the fMRI task. An FNC analysis of the IC time courses was used to examine the temporal relationship among the ICs within each condition, as well as the differences in the relationships between the 2 conditions. Tables 2 through 7 list the brain regions contained in each IC.

Results of the FNC analyses showed significant within- and between-condition correlations among the 4 ICs. These results indicate that there is a dynamic temporal interaction between basal brain activity, represented by the DMN, and how the brain responds to painful stimuli, as indicated by the 3 pain-related ICs. Fig 4 depicts the results of the within- and between-condition FNC analyses. The arrows in Fig 4 symbolize the presence of a correlation between network pairs, and the color of each arrow is an index of the lag time present in the temporal relationship from one network to another. Additionally, the direction of the arrow between each network pair indicates which network precedes the other network in time. For example, an arrow from the ISN to CCN (ISN → CCN) signifies that activity in the ISN occurred before activity in the CNN by a certain amount of time.

Fig 4A represents the FNC pattern among the 4 ICs during the NH condition. Significant temporal correlations emerged between DMN and all 3 pain-related networks (SMN, $P \leq .001$; ISN, $P \leq .001$; CCN, $P \leq .001$), with activity in pain-related networks preceding DMN activity. Additionally, there were significant temporal relationships among the pain-related networks, so that SMN preceded ISN ($P \leq .001$) and CCN ($P \leq .001$), and ISN preceded CCN ($P \leq .001$).

As shown in Fig 4B, the analysis of the RL condition revealed some consistent and unique patterns of FNC. In the RL condition, significant relationships with similar lag times to NH were found between SMN → DMN ($P \leq .001$) and ISN → DMN ($P \leq .001$) (Fig 4B). Although similar patterns were evident under RL, there were notable differences in the amount of temporal lag between multiple network pairs. For example, the overall lag times in the RL condition were longer compared to NH, and there was a significant difference in the lag time for the SMN → ISN relationship ($P \leq .001$). Additionally, there were several key differences in the temporal characteristics among the networks (ie, a change in the direction of influence) in the RL condition compared to NH. Specifically, under RL, the neural activity in the CCN preceded that of the DMN ($P \leq .001$) and the SMN ($P \leq .001$).

Fig 4C represents the significant between-condition differences among the networks' temporal correlations. When overall lag times between conditions were directly compared,

NIH-PA Author Manuscript

NIH-PA Author Manuscript

NIH-PA Author Manuscript

the only significant difference was between ISN → CCN ($P = .007$), with a significantly longer lag time for this relationship in the RL condition.

Discussion

Rectal lidocaine has been shown to significantly reduce visceral pain in IBS patients.[44] This study examined the effects of RL on 1) the coherence of the default mode network in patients with IBS and 2) the dynamic interactions between the DMN and pain-related networks via FNC analysis. Overall, the results showed that RL produced a significant change in the pain ratings and spatial patterns of the DMN in patients with IBS. Additionally, the application of RL significantly altered the temporal characteristics defining the synergy between 2 discrete pain-related networks.

DMN Functional Connectivity Under Lidocaine

The IC representing the DMN was easily identifiable in patients with IBS under both conditions, and our results suggest that this network is functionally connected with a number of pain-related brain regions not typically seen in the DMN of healthy individuals during NH. Moreover, the RL appeared to diminish these abnormalities of the DMN. Specifically, we found that the basal activity in the insula and precentral gyrus was highly coherent with, and thus incorporated into, the DMN during the NH condition. Both the insula and precentral gyrus have been associated with acute and chronic pain processing in IBS patients.[27] Previously described functions of the insula related to pain processing include self-reflection,[29] bodily arousal,[17] and bodily awareness.[22] Our results of greater DMN connectivity with the insula during NH compared to RL are consistent with findings comparing DMN connectivity between healthy controls and other chronic pain populations, including fibromyalgia[32] and diabetic neuropathy patients.[5] Napadow and colleagues[32] suggested that their findings in fibromyalgia patients demonstrate an association between increased spontaneous pain in patients and increased DMN connectivity to the insula; this association supports our results of increased pain ratings during NH. Further, the involvement of the insula with the DMN has been suggested to represent increased cognitive-emotional components of pain processing.[4] Because these areas were significantly more connected to the DMN during NH compared to RL, our results suggest that increased nociceptive pain sensitivity contributes to chronically active pain-related brain structures. Thus, the disruption of “normal” DMN connectivity may represent one possible mechanism by which pain transitions from an acute to chronic state.

Following the administration of RL, we identified several regions that showed increased functional connectivity within the DMN. Compared to NH, there was higher coherence among the middle temporal gyrus, angular gyrus, and inferior parietal lobule. These regions have previously been described as key nodes of the DMN among healthy individuals and have been associated with mental exploration[2] and episodic memory retrieval[14] and with semantic processing. Thus, the increased coherence of these regions in the DMN under RL suggests that as pain sensation is lowered, somatic focus also decreases, which in turn facilitates a pattern of DMN connectivity more consistent with pain-free individuals.

FNC

The results from this study also suggest that in addition to the changes in DMN connectivity, the pain relief provided by RL was associated with changes in the temporal characteristics, or FNC, of the DMN and other pain-related networks. In this study, we identified 3 ICs representing networks associated with discrete pain-related processes. The SMN contained subcortical structures including the thalamus, declive, substantia nigra, and culmen. These structures have been associated with receiving sensory and nociceptive input.[26,39] The ISN

NIH-PA Author Manuscript

NIH-PA Author Manuscript

NIH-PA Author Manuscript

was composed of regions associated with determining the salience of stimuli that threaten homeostasis, including the insula,[18] temporal, and somatosensory regions.[30]

The CCN contained structures associated with attention and cognitive processing of pain and included 1) the left superior frontal gyrus, which has been linked to self-reflections in decision making[11] and working memory,[13] 2) the dorsolateral prefrontal cortex, which is associated with attention to pain and pain catastrophizing,[16] and 3) the inferior parietal lobule, which is associated with active, cognitive evaluation of pain sensation.[24]

During the NH condition, patients with IBS manifested high levels of neuronal coherence among network combinations. Examination of the temporal characteristics between the DMN and the pain-related networks were consistently negatively correlated and had short lag times. Specifically, the neural activity among the pain-related networks preceded that of the DMN, and as expected, the DMN deactivated almost instantly when activity in the pain-related networks increased.

However, when sensory information related to chronic pain was attenuated via RL, there was a significant decrease in individuals' behavioral pain ratings. Additionally, the FNC results revealed that the attenuated sensory input was associated with changes in the temporal characteristics (ie, longer lag times) between pain-related network pairs. For example, the SMN → ISN relationship was slower during the RL condition, suggesting longer response time between stimulus detection and determination of salience. Because the intensity, and thus salience, of the visceral stimulus was diminished by the RL, the immediate attention and decision-making resources were less pertinent. Interestingly, the changes in temporal relationship between the ISN → CCN emerged as the only significant difference between the conditions, with RL showing a longer lag time between the 2 networks compared to NH. This result suggests that although RL resulted in longer lag times among pain-related network pairs compared to the NH condition, perhaps the crucial neural mechanism underlying the reduction of behavioral pain ratings occurs in the ISN → CCN relationship. Future studies are needed, however, before an assumption about causality can be made.

Strengths and Limitations

The DMN has previously been suggested as a potential neural marker of treatment efficacy in chronic pain,[1] and our findings now demonstrate that this network's plasticity is sensitive to treatment effects. Moreover, these results hint at several potential mechanisms involved with the onset and maintenance of central sensitization in a chronic pain population. A second strength of the study is that it appears to be the first to explore FNC between the DMN and pain-related networks in patients with IBS and in response to an analgesic. More research is needed to better understand these potential mechanisms and those that influence DMN coherence (eg, analgesics, neurotransmitters systems, and psychological variables).

Limitations to the present work are important to note. First, although our study proved valuable in understanding the temporal relationships between the DMN and pain-related networks, it is possible that patterns of DMN connectivity reflect processes associated with the experimental protocol (eg, anticipatory anxiety to painful stimuli or residual pain from the prior distension block). Future studies of DMN integrity in chronic pain populations could examine the effects of analgesics under pure resting-state conditions. A second potential criticism is the lack of a healthy control group. Although this design was ideal for addressing the goals of the original study for which data were collected,[9] the current study was a secondary data analysis. A future study designed specifically to investigate the degree to which lidocaine restores DMN functionality more consistent with a pattern seen in healthy controls is still needed. Third, the small sample size included in this study limit the

NIH-PA Author Manuscript

NIH-PA Author Manuscript

NIH-PA Author Manuscript

generalizability of findings. Finally, because the exact function of the DMN is still unclear,[8] future studies should address how treatment influences behavioral variables during fMRI data collection (such as mood and level of anxiety) and the result of these changes on DMN functionality and FNC.

Conclusion

In conclusion, our results provide evidence that the coherence of brain regions involved in the DMN is sensitive to changes in sensory input as a result of a peripheral analgesic. Additionally, RL altered the temporal relationships between the DMN and networks involved in the sensory, salience, and cognitive processing of pain. However, caution is advised in assuming that the DMN could be a potential "biomarker" for chronic pain, because neither sensitivity nor specificity of DMN activity has been established.

Acknowledgments

The authors thank the National Center for Complementary and Alternative medicine (R01AT001424, to M. Robinson) for funding their research.

References

1. Borsook D, Becerra L, Hargreaves R. Biomarkers for chronic pain and analgesia. Part 2: How, where, and what to look for using functional imaging. Discov Med. 2011; 11:209–219. [PubMed: 21447280]
2. Buckner RL, Andrews-Hanna JR, Schacter DL. The brain's default network. Ann N Y Acad Sci. 2008; 1124:1–38. [PubMed: 18400922]
3. Calhoun VD, Adali T, Pekar JJ. A method for comparing group fMRI data using independent component analysis: Application to visual, motor and visuomotor tasks. Magn Reson Imaging. 2004; 22:1181–1191. [PubMed: 15607089]
4. Canavero, S.; Bonicalzi, V. Central Pain Syndrome: Pathophysiology, Diagnosis and Management. Cambridge University Press; Cambridge: 2011.
5. Cauda F, Sacco K, Duca S, Cocito D, D'Agata F, Geminiani GC, Canavero S. Altered resting state in diabetic neuropathic pain. PLoS One. 2009; 4:e4542. [PubMed: 19229326]
6. Christoff K, Gordon AM, Smallwood J, Smith R, Schooler JW. Experience sampling during fMRI reveals default network and executive system contributions to mind wandering. Proc Natl Acad Sci U S A. 2009; 106:8719–8724. [PubMed: 19433790]
7. Cifre I, Sitges C, Fraiman D, Muñ MÁ, Balenzuela P, González-Roldán A, Martínez-Jauand M, Birbaumer N, Chialvo DR, Montoya P. Disrupted functional connectivity of the pain network in fibromyalgia. Psychosom Med. 2012; 74:55–62. [PubMed: 22210242]
8. Cole DM, Smith SM, Beckmann CF. Advances and pitfalls in the analysis and interpretation of resting-state fMRI data. Front Syst Neurosci. 2010; 4:8. [PubMed: 20407579]
9. Craggs JG, Price DD, Verne GN, Perlstein WM, Robinson ME. Functional brain interactions that serve cognitive–affective processing during pain and placebo analgesia. Neuroimage. 2007; 38:720–729. [PubMed: 17904390]
10. Davis KD. Neuroimaging of pain: What does it tell us? Curr Opin Support Palliat Care. 2011; 5:116–121. [PubMed: 21415755]
11. Deppe M, Schwindt W, Kugel H, Plassmann H, Kenning P. Nonlinear responses within the medial prefrontal cortex reveal when specific implicit information influences economic decision making. J Neuroimaging. 2005; 15:171–182. [PubMed: 15746230]
12. Deshpande, G.; Kerssens, C.; Huo, X.; Hu, X. Simultaneous investigation of local and distributed functional brain connectivity from fMRI data; Neural Engineering 5th International IEEE/EMBS; 2011; p. 57-63.

NIH-PA Author Manuscript

NIH-PA Author Manuscript

NIH-PA Author Manuscript

13. Du Boisgueheneuc F, Levy R, Volle E, Seassau M, Duffau H, Kinkingnehun S, Samson Y, Zhang S, Dubois B. Functions of the left superior frontal gyrus in humans: A lesion study. Brain. 2006; 129:3315–3328. [PubMed: 16984899]

14. Fransson P, Marrelec G. The precuneus/posterior cingulate cortex plays a pivotal role in the default mode network: Evidence from a partial correlation network analysis. Neuroimage. 2008; 42:1178–1184. [PubMed: 18598773]

15. Genovese CR, Lazar NA, Nichols T. Thresholding of statistical maps in functional neuroimaging using the false discovery rate. Neuroimage. 2002; 15:870–878. [PubMed: 11906227]

16. Gracely RH, Geisser ME, Giesecke T, Grant MA, Petzke F, Williams DA, Clauw DJ. Pain catastrophizing and neural responses to pain among persons with fibromyalgia. Brain. 2004; 127:835–843. [PubMed: 14960499]

17. Gray MA, Harrison NA, Wiens S, Critchley HD. Modulation of emotional appraisal by false physiological feedback during fMRI. PLoS One. 2007; 2:e546. [PubMed: 17579718]

18. Grinband J, Hirsch J, Ferrera VP. A neural representation of categorization uncertainty in the human brain. Neuron. 2006; 49:757–763. [PubMed: 16504950]

19. Gusnard DA, Akbudak E, Shulman GL, Raichle ME. Medial prefrontal cortex and self-referential mental activity: Relation to a default mode of brain function. Proc Natl Acad Sci U S A. 2001; 98:4259–4264. [PubMed: 11259662]

20. Hall GBC, Kamath MV, Collins S, Ganguli S, Spaziani R, Miranda KL, Bayati A, Bienenstock J. Heightened central affective response to visceral sensations of pain and discomfort in IBS. Neurogastroenterol Motil. 2010; 22:276–e280. [PubMed: 20003075]

21. Jafri MJ, Pearlson GD, Stevens M, Calhoun VD. A method for functional network connectivity among spatially independent resting-state components in schizophrenia. Neuroimage. 2008; 39:1666–1681. [PubMed: 18082428]

22. Karnath HO, Baier B, Nägele T. Awareness of the functioning of one's own limbs mediated by the insular cortex? J Neurosci. 2005; 25:7134–7138. [PubMed: 16079395]

23. Kellow JE, Delvaux M, Azpiroz F, Camilleri M, Quigley EM, Thompson DG. Principles of applied neurogastroenterology: Physiology/motility-sensation. Gut. 1999; 45:II17–II24. [PubMed: 10457040]

24. Kong J, White NS, Kwong KK, Vangel MG, Rosman IS, Gracely RH, Gollub RL. Using fMRI to dissociate sensory encoding from cognitive evaluation of heat pain intensity. Hum Brain Map. 2006; 27:715–721.

25. Lorenzi M, Beltramello A, Mercuri NB, Canu E, Zoccatelli G, Pizzini FB, Alessandrini F, Cotelli M, Rosini S, Costardi D, Caltagirone C, Frisoni GB. Effect of memantine on resting state default mode network activity in Alzheimer's disease. Drugs Aging. 2011; 28:205–217. [PubMed: 21250762]

26. Lu CL, Wu YT, Yeh TC, Chen LF, Change FY, Lee SE, Ho LT, Hsieh JC. Neuronal correlates of gastric pain induced by fundus distension: A 3T-fMRI study. Neurogastroenterol Motil. 2004; 16:575–587. [PubMed: 15500514]

27. Mayer EA, Berman S, Suyenobu B, Labus J, Mandelkern MA, Naliboff BD, Chang L. Differences in brain responses to visceral pain between patients with irritable bowel syndrome and ulcerative colitis. Pain. 2005; 115:398–409. [PubMed: 15911167]

28. Mertz H, Naliboff B, Munakata J, Niazi N, Mayer EA. Altered rectal perception is a biological marker of patients with irritable bowel syndrome. Gastroenterology. 1995; 109:40–52. [PubMed: 7797041]

29. Modinos G, Ormel J, Aleman A. Activation of anterior insula during self-reflection. PLoS One. 2009; 4:e4618. [PubMed: 19242539]

30. Moulton EA, Pendse G, Becerra LR, Borsook D. BOLD responses in somatosensory cortices better reflect heat sensation than pain. J Neurosci. 2012; 32:6024–6031. [PubMed: 22539862]

31. Naliboff BD, Munakata J, Fullerton S, Gracely RH, Kodner A, Harraf F, Mayer EA. Evidence for two distinct perceptual alterations in irritable bowel syndrome. Gut. 1997; 41:505–512. [PubMed: 9391250]

NIH-PA Author Manuscript

NIH-PA Author Manuscript

NIH-PA Author Manuscript

32. Napadow V, LaCount L, Park K, As-Sanie S, Clauw DJ, Harris RE. Intrinsic brain connectivity in fibromyalgia is associated with chronic pain intensity. Arthritis Rheum. 2010; 62:2545–2555. [PubMed: 20506181]
33. Otti A, Guendel H, Henningsen P, Zimmer C, Wohlschlaeger AM, Noll-Hussong M. Functional network connectivity of pain-related resting state networks in somatoform pain disorder: An exploratory fMRI study. J Psychiatry Neurosci. 2012; 38:57–65. [PubMed: 22894821]
34. Peterson BS, Potenza MN, Wang Z, Zhu H, Martin A, Marsh R, Plessen KJ, Yu S. An fMRI study of the effects of psychostimulants on default-mode processing during Stroop task performance in youths with ADHD. Am J Psychiatry. 2009; 166:1286–1294. [PubMed: 19755575]
35. Saab C: Visualizing the complex brain dynamics of chronic pain. J Neuroimmune Pharmacol. 2012
36. Sambataro F, Blasi G, Fazio L, Caforio G, Taurisano P, Romano R, Di Giorgio A, Gelao B, Bianco LL, Papazacharias A, Popolizio T, Nardini M, Bertolino A. Treatment with olanzapine is associated with modulation of the default mode network in patients with Schizophrenia. Neuropsychopharmacology. 2009; 35:904–912. [PubMed: 19956088]
37. Seifert F, Maihöfner C. Functional and structural imaging of pain-induced neuroplasticity. Curr Opin Anesthesiol. 2011; 24:515–523.
38. Seminowicz DA, Davis KD. Pain enhances functional connectivity of a brain network evoked by performance of a cognitive task. J Neurophysiol. 2007; 97:3651–3659. [PubMed: 17314240]
39. Starr CJ, Sawaki L, Wittenberg GF, Burdette JH, Oshiro Y, Quevedo AS, McHaffie JG, Coghill RC. The contribution of the putamen to sensory aspects of pain: Insights from structural connectivity and brain lesions. Brain. 2011; 134:1987–2004. [PubMed: 21616963]
40. Tagliazucchi E, Balenzuela P, Fraiman D, Chialvo DR. Brain resting state is disrupted in chronic back pain patients. Neurosci Lett. 2010; 485:26–31. [PubMed: 20800649]
41. Tillisch K, Larsson MB, Kilpatrick LA, Engstrom M, Naliboff BD, Lundberg P, Walter SA, Mayer EA. Women with irritable bowel syndrome (IBS) show altered default mode network connectivity. Gastroenterology. 2011; 140:S-364.
42. Vase L, Robinson ME, Verne GN, Price DD. The contributions of suggestion, desire, and expectation to placebo effects in irritable bowel syndrome patients: An empirical investigation. Pain. 2003; 105:17–25. [PubMed: 14499416]
43. Verne GN, Himes NC, Robinson ME, Gopinath KS, Briggs RW, Crosson B, Price DD. Central representation of visceral and cutaneous hypersensitivity in the irritable bowel syndrome. Pain. 2003; 103:99–110. [PubMed: 12749964]
44. Verne GN, Sen A, Price DD. Intrarectal lidocaine is an effective treatment for abdominal pain associated with diarrhea-predominant irritable bowel syndrome. J Pain. 2005; 6:493–496. [PubMed: 16084463]
45. Wartolowska K. How neuroimaging can help us to visualise and quantify pain? Eur J Pain Suppl. 2011; 5:323–327.
46. Whitehead WE, Holtkotter B, Enck P, Hoelzl R, Holmes KD, Anthony J, Shabsin HS, Schuster MM. Tolerance for rectosigmoid distention in irritable bowel syndrome. Gastroenterology. 1990; 98:1187–1192. [PubMed: 2323511]

NIH-PA Author Manuscript

NIH-PA Author Manuscript

NIH-PA Author Manuscript

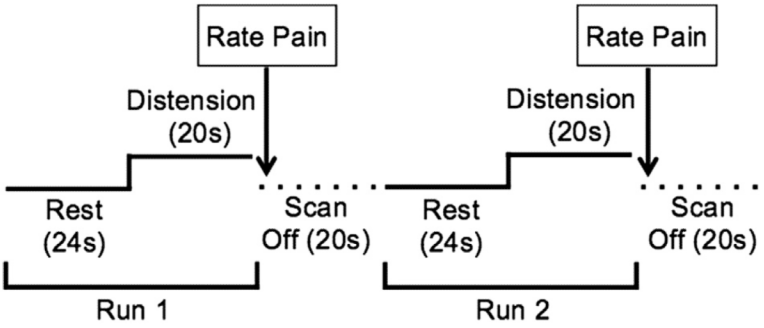

Figure 1.
The functional magnetic resonance imaging scanning session consisted of seven 44-s runs, with 24 s of rest and 20 s of rectal balloon distension. Pain ratings were collected at the end of each run, and participants were given 20 s before the start of the subsequent run. An example of the first 2 runs is portrayed above.

NIH-PA Author Manuscript

NIH-PA Author Manuscript

NIH-PA Author Manuscript

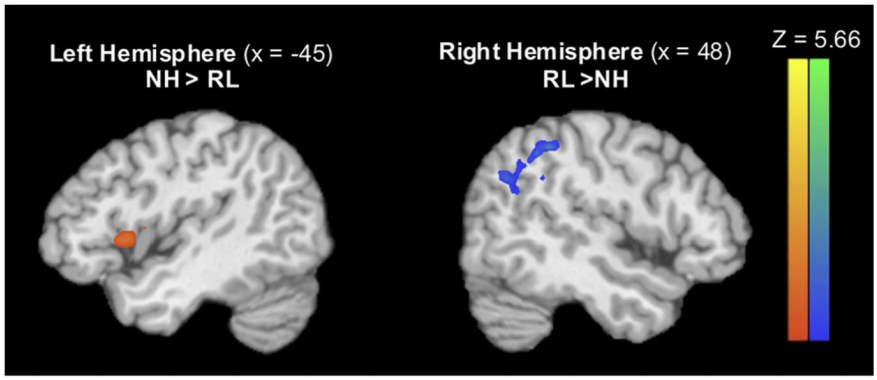

Figure 2.

Significant differences ($P \leq .05$, FDR $\leq .05$) between the NH and RL conditions emerged in the regions functionally connected with the DMN. Regions identified as significantly more connected with the DMN in NH include the insula and precentral gyrus (*orange, pictured left*), whereas the superior and middle temporal gyri, angular gyrus, and inferior parietal lobule were significantly more connected with the DMN in RL (*blue, pictured left*). Abbreviation: FDR, false discovery rate.

NIH-PA Author Manuscript

NIH-PA Author Manuscript

NIH-PA Author Manuscript

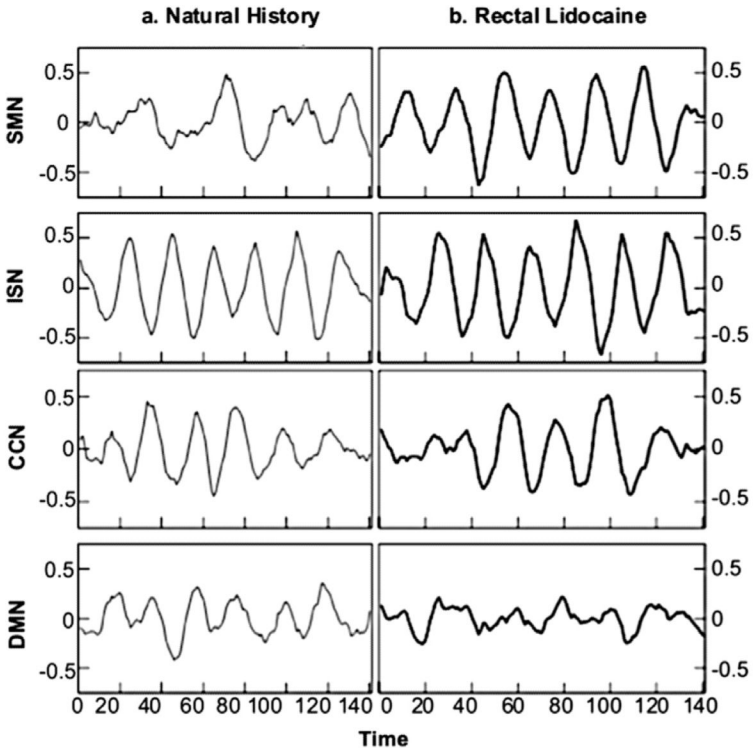

Figure 3.

Lag times reported in the FNC analyses were calculated based on the time courses of the DMN and 3 pain-processing networks (SMN, ISN, and CCN). The waveforms represent each IC's time course, or pattern of activation, over the period of the fMRI task. Time courses from the ICs in the NH condition are shown on the left, and time courses from the ICs in the RL condition are shown on the right.

NIH-PA Author Manuscript
NIH-PA Author Manuscript
NIH-PA Author Manuscript

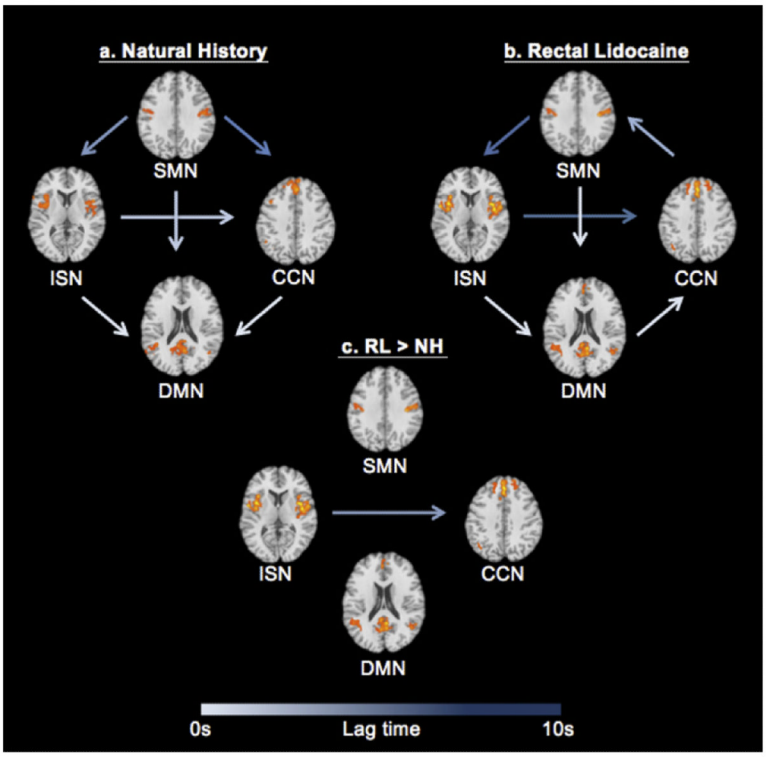

Figure 4.

The temporal relationships between the DMN and pain-related neural networks (ie, ICs) are represented above. Arrows represent the presence of a correlation between network pairs, and lag times are denoted by arrow color, with longer lag times displayed in darker arrow colors. The direction of the arrow indicates that one network precedes another network by a certain amount of time. For example, ISN → CCN shows that the ISN precedes the CCN. Significant correlations were present among all network pairs in both the NH and RL conditions (left and right, respectively). The only significant condition-level differences were found for the ISN → CCN relationship (center). In the RL condition, the CCN lagged the ISN significantly more than in the NH condition ($P \leq .05$, FDR ≤ .05). All images are in radiologic convention, and Z-plane coordinates for each network are located at SMN = 32, CCN = 38; ISN = 7, DMN = 18. Abbreviation: FDR, false discovery rate.

NIH-PA Author Manuscript

NIH-PA Author Manuscript

NIH-PA Author Manuscript

Table 1

Significant Differences in Functionally Connected Regions to the DMN, Based on Condition ($P \leq .05$, FDR ≤ .05)

			TAL Coordinates				
Condition	*Region*	*Brodmann Area*	*X*	*Y*	*Z*	*Peak Z-Score*	*Cluster Size*
NH >RL	Left insula	13	−47	12	6	3.64	52
	Left precentral gyrus	43	−54	−7	13	2.82	7
RL >NH	Right superior temporal gyrus	39	42	−58	27	5.66	81
	Right middle temporal gyrus	39	48	−66	26	3.53	9
	Right angular gyrus	39	56	−63	31	4.33	12
	Right inferior parietal lobule	40	47	−46	40	4.72	23

Abbreviation: TAL, Talairach.

NIH-PA Author Manuscript

NIH-PA Author Manuscript

NIH-PA Author Manuscript

Table 2
Regions Comprising the SMN in the NH Condition ($P \leq .05$, FDR ≤ .05)

		TAL Coordinates				
Region	Brodmann Area	X	Y	Z	Peak Z-Score	Cluster Size
Left postcentral gyrus	43	−53	−10	22	3.07	56
Right postcentral gyrus	2	39	−25	39	3.06	67
	43	65	−16	14	3.85	34
Right insula	13	45	−15	19	2.93	156
Right precuneus	7	7	−45	51	3.20	17
	19	33	−71	36	3.42	24
Left inferior parietal lobule	39	−36	−63	38	3.2.88	40
Right inferior parietal lobule	40	39	−36	51	3.09	45
Right thalamus		12	−18	7	3.28	39
Right declive		34	−58	−7	3.12	15
Right culmen		0	−36	−19	3.55	28
Right caudate		20	−2	28	3.04	16
Left middle frontal gyrus	6	−4	−15	62	2.70	31
	8	−22	22	47	3.02	18
Right middle frontal gyrus	8	15	31	44	2.97	17
Left cingulate gyrus	24	−7	−14	41	2.87	46
Right cingulate gyrus	32	18	14	39	3.07	23
Left superior temporal gyrus	13	−34	−46	13	2.96	15
	41	−42	−29	14	2.81	24
Right superior temporal gyrus	22	51	−14	6	3.14	643
	41	50	−32	16	3.00	41
Right inferior frontal gyrus	9	53	5	30	3.21	46
Left paracentral lobule	5	−19	−32	50	3.21	46
Left precentral gyrus	3	−33	−28	45	2.85	68
	4	−36	−17	37	2.99	207
Right precentral gyrus	4	28	−29	44	2.92	35
	6	10	−18	65	3.02	53
Left substantia nigra		−11	−23	−6	3.25	16
Right cuneus	17	19	−72	8	2.70	35
Right parahippocampal gyrus	19	27	−43	−1	3.07	16

Abbreviations: FDR, false discovery rate; TAL, Talairach.

NIH-PA Author Manuscript

NIH-PA Author Manuscript

NIH-PA Author Manuscript

Table 3
Regions Comprising the SMN in the RL Condition ($P \leq .05$, FDR ≤ .05)

		TAL Coordinates				
Region	Brodmann Area	X	Y	Z	Peak Z-Score	Cluster Size
Left postcentral gyrus	3	−41	−20	35	3.22	933
	43	−53	−13	15	3.81	27
Right postcentral gyrus	2	40	−22	31	3.38	925
	3	62	−14	26	4.32	79
Left insula	13	−42	−15	17	3.17	105
Right insula	13	48	−18	19	3.44	151
Right precuneus	7	25	−41	43	3.06	40
	19	36	−66	37	3.05	1.9
Right inferior parietal lobule	40	42	−40	38	2.98	34
Left thalamus		−19	−23	18	2.89	21
Left declive		−19	−68	−9	2.92	34
Right declive		21	−59	−12	2.99	21
Right culmen		0	−34	−17	3.80	29
Left caudate		−20	8	24	2.90	26
Left middle frontal gyrus	6	−28	16	49	2.92	24
Right middle frontal gyrus	6	7	−18	50	2.96	97
Left cingulate gyrus	24	−7	−11	39	3.06	21
Left superior temporal gyrus	41	−40	−34	14	3.44	24
Left inferior frontal gyrus	45	−44	35	4	2.70	36
	47	−41	16	−14	2.34	32
Left paracentral lobule	6	−3	−29	58	2.90	25
Left middle temporal gyrus	39	−31	−67	28	2.75	19
Right middle temporal gyrus	39	45	−66	22	3.04	55
Left superior frontal gyrus	6	−8	8	55	2.81	31
Right superior frontal gyrus	6	18	22	65	2.97	20

Abbreviations: FDR, false discovery rate; TAL, Talairach.

NIH-PA Author Manuscript

NIH-PA Author Manuscript

NIH-PA Author Manuscript

Table 4
Regions Comprising the ISN in the NH Condition (P ≤ .05, FDR ≤ .05)

		TAL Coordinates				
Region	***Brodmann Area***	***X***	***Y***	***Z***	***Peak Z-Score***	***Cluster Size***
Left insula	13	−42	−17	14	3.84	85
Right insula	13	34	−7	17	3.96	746
Left cingulate gyrus	32	−4	12	36	3.98	59
Left superior temporal gyrus	22	−55	−46	14	3.98	18
Right superior temporal gyrus	22	56	−46	13	3.84	29
Right precentral gyrus	44	46	−2	9	4.40	69
Left postcentral gyrus	40	−58	−27	23	3.92	80
Left inferior frontal gyrus	44	−60	7	14	4.10	645
Left inferior parietal lobule	40	−57	−38	25	3.50	20
Right inferior parietal lobule	40	58	−36	24	4.00	118
Right superior parietal lobule	7	15	−51	61	3.94	56
Left claustrum		−34	−5	8	4.27	159
Right claustrum		32	8	−3	5.45	18
Right transverse temporal gyrus	41	40	−20	12	4.22	39
Right middle temporal gyrus	19	45	−58	15	3.81	48

Abbreviations: FDR, false discovery rate; TAL, Talairach.

NIH-PA Author Manuscript

NIH-PA Author Manuscript

NIH-PA Author Manuscript

Table 5

Regions Comprising the ISN in the RL Condition ($P \leq .05$, FDR ≤ .05)

		TAL Coordinates				
Region	Brodmann Area	X	Y	Z	Peak Z-Score	Cluster Size
Left insula	13	−38	−3	13	4.25	858
Right insula	13	40	−13	3	4.39	1121
Right cingulate gyrus	24	3	12	31	4.24	223
Left superior temporal gyrus	22	−59	−3	6	5.97	26
Right superior temporal gyrus	13	53	−44	20	4.34	20
	22	61	−52	9	3.97	27
	39	45	−52	22	3.78	29
Left precentral gyrus	13	−48	−9	13	5.23	36
Left postcentral gyrus	40	−50	−24	16	4.21	101
Right postcentral gyrus	43	51	−12	17	4.03	116
Right inferior frontal gyrus	44	52	0	16	5.15	29
Right inferior parietal lobule	40	56	−33	22	4.56	33
Right precuneus	31	9	−69	18	4.05	71
Right lentiform nucleus		31	−4	1	5.02	30

Abbreviations: FDR, false discovery rate; TAL, Talairach.

NIH-PA Author Manuscript

NIH-PA Author Manuscript

NIH-PA Author Manuscript

Table 6
Regions Comprising the CCN in the NH Condition ($P \leq .05$, FDR ≤.05)

		TAL Coordinates				
Region	Brodmann Area	X	Y	Z	Peak Z-Score	Cluster Size
Left superior frontal gyrus	6	−2	8	58	3.75	137
	8	−2	37	44	5.64	23
	9	−19	43	38	5.10	41
Right superior frontal gyrus	6	15	25	52	4.38	26
	9	19	46	35	3.87	29
	10	29	49	27	4.07	44
Left middle frontal gyrus	6	−47	8	43	4.07	198
	8	−4	46	38	4.19	1044
	9	−45	11	35	3.99	35
Right middle frontal gyrus	6	15	14	57	4.27	52
	8	15	34	44	3.78	21
	9	54	18	30	3.76	50
Left insula	13	−47	9	3	3.44	20
Right superior temporal gyrus	22	44	−55	15	3.53	30
Left precuneus	31	−3	−46	30	3.83	32
Left inferior frontal gyrus	44	−53	13	16	3.89	27
Left middle temporal gyrus	39	−48	−63	25	3.94	20
Left inferior parietal lobule	39	−41	−63	40	3.88	43
	40	−55	−54	38	3.83	156
Left supramarginal gyrus	40	−53	−52	25	4.02	27
Right supramarginal gyrus	40	53	55	37	3.53	37
Right uvula		29	−71	−23	4.46	44

Abbreviations: FDR, false discovery rate; TAL, Talairach.

NIH-PA Author Manuscript

NIH-PA Author Manuscript

NIH-PA Author Manuscript

Table 7

Regions Comprising the CCN in the RL Condition ($P \leq .05$, FDR ≤ .05)

		TAL Coordinates				
Region	*Brodmann Area*	*X*	*Y*	*Z*	*Peak Z-Score*	*Cluster Size*
Left superior frontal gyrus	6	−19	22	52	5.20	166
	9	−4	47	30	5.30	710
Right superior frontal gyrus	6	7	20	54	5.26	65
	10	23	46	55	4.88	45
Left middle frontal gyrus	6	−50	8	49	5.18	23
	8	−41	9	43	5.11	89
Right middle frontal gyrus	6	15	13	42	4.37	45
Left precuneus	31	−3	46	30	4.13	71
Left insula	13	−42	12	0	3.98	151
Left superior temporal gyrus	39	−47	−60	30	4.04	193

Abbreviations: FDR, false discovery rate; TAL, Talairach.